



Politecnico di Torino

Master Degree in Electrical Engineering

A.Y. 2021/2022

July 2022

Low Frequency Dosimetry Including Nerve Stimulation Modelling

Supervisors:

Fabio Freschi

Luca Giaccone

Student:

Mustapha Ez Zarzouri - 264595

Contents

1	Introduction	2
2	Model for Excitation of Myelinated Nerve	4
2.1	Nerves "excitable cells"	4
2.2	ionic current	5
2.2.1	The Nernst Equation	7
2.3	Membrane equivalent circuit	9
2.4	Action potential	14
3	Impulse Propagation	16
3.1	Mathematical model	16
3.2	External Voltage Source ϕ_e	19
3.3	Spatially Extended Nonlinear Node	20
3.3.1	SENN Implementation	21
3.3.2	SENN Model Results	22
4	Model Simulation	28
4.1	modified SENN	28
4.1.1	Code Implementation	29
4.2	Modified SENN application	31
4.2.1	21-node axon model response	31
4.2.2	3D-body model	33
4.2.3	Y-model response	35

5	3D Modeling	41
5.1	Medial Axis	42
5.2	Skeletonization algorithm	42
6	Conclusion	44

List of Figures

2.1	Neuron's structure	4
2.2	Example of spinal nerve	5
2.3	Cell membrane	7
2.4	Equivalent Circuit (HH parallel-Conductance model)	10
2.5	Action potential	15
3.1	Circuit Model	17
3.2	Nerve Model	20
3.3	Sub-threshold response	23
3.4	Node-13 Sub-threshold response	24
3.5	Node-11 threshold response	25
3.6	adjacent nodes threshold response	26
3.7	Node-11 Supra-threshold response	27
4.1	Node-11 linear vs nonlinear comparison	32
4.2	Nodes 12 to 15 comparison, lines: nonlinear; circles: linear	33
4.3	3D-Cylinder Model	34
4.4	3D-Cylinder Model	34
4.5	Y Model skeleton	35
4.6	Sub-threshold stimulus result	37
4.7	Threshold stimulus result	38
4.8	sopra-threshold stimulus result	39
4.9	Adjacent nodes - sopra-threshold stimulus result .	39
4.10	distant nodes	40

List of Tables

2.1	Ionic Concentrations	6
2.2	Constants for FH equations	13
3.1	Input Parameters	21

Abstract

Many models have been presented in the literature, since 50s, which describe very well the behavior of nerve fibers, all of them are based on Hodgkin and Huxley's work (1952). In this thesis a particular attention was given to SENN model (spatially extended nonlinear node), it was analyzed and then extended further to include nonlinear Frankenhaeuser and Huxley equations in all nodes. The new model obtained is easily implementable, applicable to different nerve's structures and works with multiple classes of external stimuli.

The second part of the thesis focuses on 3D-modelling. A special algorithm is used to identify the nerve voxels from a 3D body model and then approximate the structure topology with the centerline.

To conclude, the model was tested using, as stimulus, a magnetic field generated by an external coil to simulate a body exposure to an external magnetic field.

Chapter 1

Introduction

Electromagnetic dosimetry deals with the determination of dosimetric quantities using experimental, analytical or numerical techniques. The latter showed the greatest potential and have led to the development of various commercial software that flank the programs developed in research areas. The main purpose is to assess the health risks associated with exposure to electromagnetic fields and more, these techniques are also used to optimize the design of magnetic resonance machines.

The goal of this thesis work is to implement a neuro-dynamic model for numerical simulation based on models already existing in the literature, with the aim of evaluating the excitation threshold, capable of generating an action potential, in nerve cells in response to an external stimulus. Exceeding the threshold can mean, for a person, an involuntary movement or it can generate sensations of pain or discomfort. To do all this, first of all, research was done to understand the functioning of excitable cells, all the researches lead back to the extraordinary work of two English physiological scientists, Huxley and Hodgkin, who thanks to their work won the nobel prize. In the 1950s they managed to create a mathematical model that describes the mechanism of nerve cells, by experimenting on an axon of a giant squid, their model is still used today. After which reilly's neuro-electric model was used

which, using the equations of Frankenhaeuser and Huxley, defined a circuit model of a nerve and studied the response to different types of stimuli.

In this thesis work, reilly's model was taken and extended to a more generic case, introducing the equations of F-H in all nodes of the nervous model, drawing some advantages, including ease of implementation, but this move also brings with it the disadvantage of the increased computational cost. Finally, the neuro electric model was tested on a simple 3-D geometry case. concentric cylinders were used to simulate parts of a body (as arms or legs). It was necessary to trace back to the use of image processing algorithms in order to integrate the 1-D neuro electric model into the discrete 3-D model.

Chapter 2

Model for Excitation of Myelinated Nerve

2.1 Nerves "excitable cells"

In this chapter a brief description of the functioning of excitable cells is given.

Nervous tissue is the main component of the nervous system, it is composed by Neurons and Neuroglia. Neurons are known as excitable cells which can receive and transmit impulses. While Neuroglia assist the propagation of the nerve impulse and provide nutrients to the neurons.

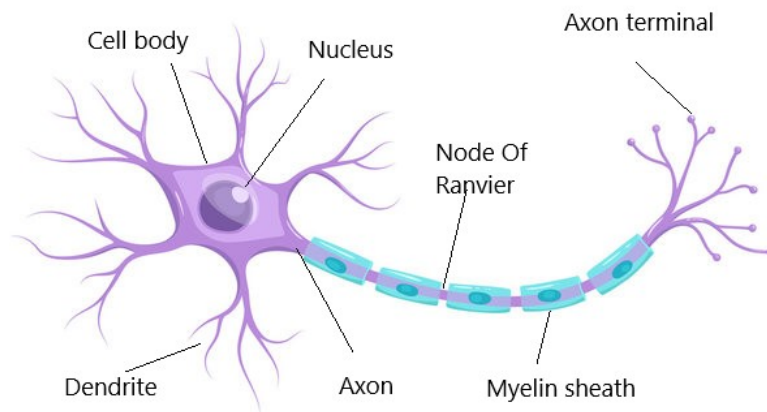


Figure 2.1: Neuron's structure

The central part of neuron is called cell body, which contains the nucleus, Figure 2.1. Projecting from the cell body we can see many branches called dendrites which are responsible for receiving electrochemical stimulations from other neural cells and propagate them to the cell body. Finally we have the axon which carry the action potential from the cell toward the next neuron. For many neurons, the axon account for the majority of the length of the cell, sometimes extending long distances ($> 1m$) at which point we can call them nerve fibers. Many fibers are bounded together to form a nerve fascicle which in turn are grouped together to form nerves as shown in Figure:2.2

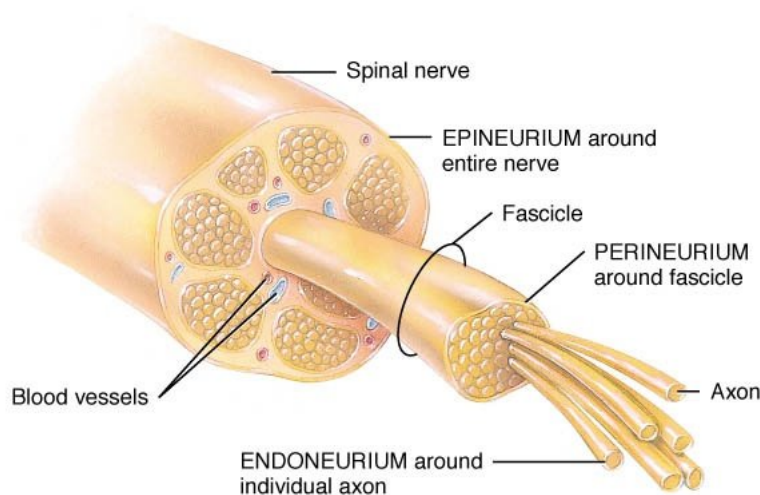


Figure 2.2: Example of spinal nerve

2.2 ionic current

To understand how a membrane potential occurs we need to consider the chemicals on either sides of the cell membrane, the outside of each cell is bathed in a sodium chloride solution made of positively charged sodium ions and negatively charged chloride ions. Inside the cell, in contact with the cell membrane are positively charged potassium ions, negatively charged phosphate ions

and anionic proteins. The presence of electric charges both inside and outside the cell, separated from the membrane and with different concentrations, generates a difference in electrical potential. The electrical balance is altered when ions selectively pass through the cell membrane to the other side generating a change in membrane potential.

For all excitable cells the concentration of intracellular potassium greatly exceeds extracellular one. On the other hand, we have a significant concentration of sodium and chloride ions outside the cell respect to the inside. Table 2.1 shows an example of ionic concentrations for nerve axon.

<i>Nerve (squid axon)</i>		
	<i>Intracellular [mM]</i>	<i>Extracellular [mM]</i>
K^+	397	20
Na^+	50	437
Cl^-	40	556

Table 2.1: Ionic Concentrations

The membrane is said to be semipermeable, it is a dielectric insulator that permits the passage of some ions through the so-called ion channels Figure 2.3. The individual channels may be very selective with respect to the ionic species that are allowed to pass. There are four types of channels through which ions might pass, leak channels, that are typically always open, chemically-gated channel, voltage-gated channel and mechanically-gated channel. Gated channel must open their gate to allow the passage of ions.

Ions passively diffuse through a channel from higher to lower concentration they also attracted/repelled by opposite/like charges from other charged molecules thus the direction of ion's flow depends on the balance between both electrical and chemical forces acting on the ion at any given time. A quantitative description of this phenomena is given by the Nernst Equation.

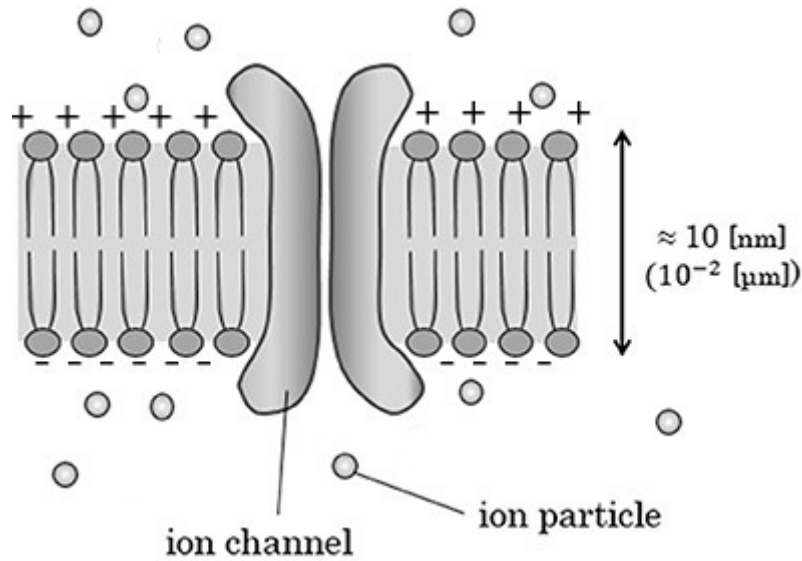


Figure 2.3: Cell membrane

2.2.1 The Nernst Equation

The Nernst equation relates the flow of ions to spatial differences in concentration or in electric potential. In a solution with a different spacial distribution of particles there will be a net ion flux down the concentration gradient.

If we consider the the concentration potential energy difference W_c , that is the work needed to move a mole of S (S represent a concentration of a generic substance) against the gradient we can say that this quantity is proportional to the logarithm of the concentration difference in according to 2.1

$$W_c = RT(\ln[S]_i - \ln[S]_o) \quad (2.1)$$

$$W_c = RT \ln \frac{[S]_i}{[S]_o} \quad (2.2)$$

Where:

- $[S]_i$ and $[S]_o$ represent the inside and outside concentration respectively.

- R is the gas constant.
- T is the absolute temperature.

If the particles are electrically charged, there will be a difference in electric potential between regions with different concentrations. The electrical potential energy that will be obtained is given by the relation 2.3

$$\mathbf{W_e} = \mathbf{ZFV_m} \quad (2.3)$$

Where:

- Z is the valence of S.
- F is the Faraday constant.
- V_m is the membrane potential.

The total potential energy difference (ΔW) is the sum of 2.2 and 2.3. At the equilibrium, when $\Delta W = 0$ we obtain the so-called Nernst Equation 2.4

$$\mathbf{V_m} = \frac{\mathbf{RT}}{\mathbf{FZ}} \ln \frac{[\mathbf{S}]_o}{[\mathbf{S}]_i} \quad (2.4)$$

In case of presence of more substances the equation becomes 2.5

$$\mathbf{V_m} = \frac{\mathbf{RT}}{\mathbf{FZ}} \ln \left(\frac{\mathbf{P_{S_1}}[\mathbf{S_1}]_o + \mathbf{P_{S_2}}[\mathbf{S_2}]_o}{\mathbf{P_{S_1}}[\mathbf{S_1}]_i + \mathbf{P_{S_2}}[\mathbf{S_2}]_i} \right) \quad (2.5)$$

Where P_{S_i} is the permeability of the i-th substance.

A numerical example if we suppose the membrane permeable to potassium ions but to no others and using the values $R = 8.3144 \frac{J}{K.mole}$, $T = 295.18K$, $F = 96.5 \frac{C}{g.mole}$, $[K^+]_o = 2.5mM$, $[K^+]_i = 120mM$ and $Z = +1$ (for a monovalent cation):

$$\mathbf{V_m} = \frac{\mathbf{RT}}{\mathbf{FZ}} \ln \frac{[\mathbf{K^+}]_o}{[\mathbf{K^+}]_i} = -98mV \quad (2.6)$$

This value is called the equilibrium potential of potassium we will refer to it using the symbol E_k .

We can do the same think with the sodium, we get $E_{Na} = 55mV$. Combining all ions together and using 2.5 we get the Rest Potential¹ of the membrane:

$$V_{rest} = \frac{RT}{F} \ln \left(\frac{P_K[K]_o + P_{Na}[Na]_o + P_{Cl}[Cl]_i}{P_K[K]_i + P_{Na}[Na]_i + P_{Cl}[Cl]_o} \right) \approx -70mV \quad (2.7)$$

2.3 Membrane equivalent circuit

As we said before the cell membrane is a dielectric insulator which separates the negative electric charges inside from the positive ones outside. The thickness of the membrane is very small compared to the size of the cell, we are talking about tens of nanometers, considering a membrane potential ($\approx 100mV$) the electric field developed across the membrane is about ($\approx 10^7 \frac{V}{m}$). One important aspect of the cell membrane is its capacitance, it can be represented in the equivalent electric circuit by a capacitor. The value of this capacitor, of roughly $2\mu F/cm^2$, is extremely high compared to most materials used in ordinary factory-made capacitors.

Hodgkin and Huxley (1952) provided the first detailed description of electrical proprieties of the excitable membrane of unmyelinated nerve cells. This work was extended later by Frankenhaeuser and Huxley (1964) to describe the myelinated nerve membrane. In Fig 2.4 we refer to the HH parallel-Conductance model [6].

The electrical model consists of membrane capacitance, nonlinear conductances for Na^+ and K^+ and a linear leakage element.

¹the contribution of the chloride current is negligible compared to the other two.

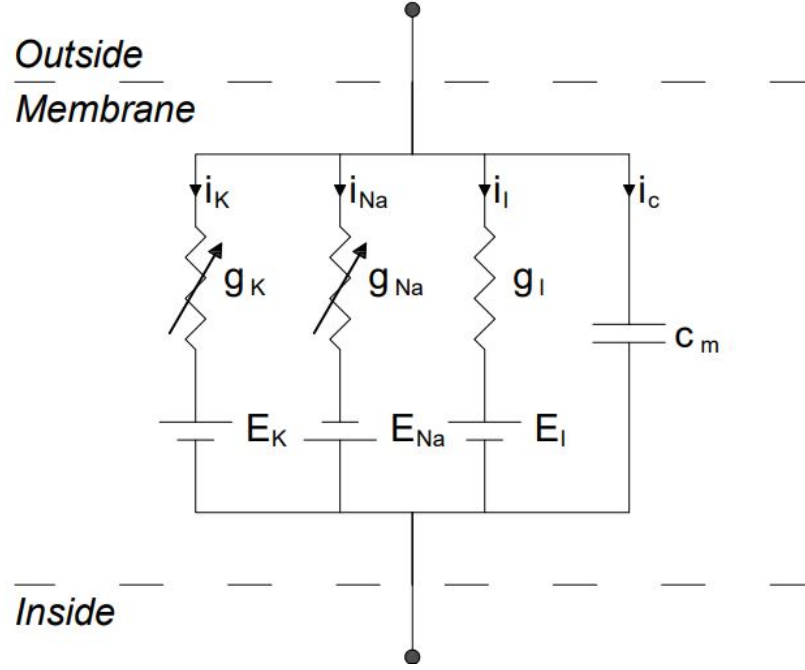


Figure 2.4: Equivalent Circuit (HH parallel-Conductance model)

The set of HH equations is given by:

$$\mathbf{i}_m = c_m \frac{dV_m}{dt} + (\mathbf{i}_{Na} + \mathbf{i}_k + \mathbf{i}_l) \quad (2.8)$$

Where i_m is the membrane current, c_m is the membrane capacity, V_m is the membrane voltage, and i_{Na} , i_k , and i_l are the ionic current.

The ionic terms are expressed by[6]:

$$\mathbf{i}_{Na} = g_{Na}(V_m - E_{Na}) \quad (2.9)$$

$$\mathbf{i}_K = g_K(V_m - E_K) \quad (2.10)$$

$$\mathbf{i}_l = g_l(V_m - E_l) \quad (2.11)$$

Where g_{Na} , g_K and g_l are the ionic conductances, and E_{Na} , E_K , and E_l are the ionic Nernst potentials. g_l is a linear conduc-

tance while g_{Na} and g_K are described by two nonlinear functions of the form:

$$g_{Na} = \bar{g}_{Na} m^3 h \quad (2.12)$$

$$g_K = \bar{g}_K n^4 \quad (2.13)$$

where \bar{g}_{Na} and \bar{g}_K represent the maximum conductance values, and m , n , and h are so-called activation and deactivation variables that modulate the maximum conductances.

In this work we refer to the Frankenhaeuser and Huxley model (FH) [1] that describe better the myelinated nerve membrane. The difference between the two models is that in the FH-model the ionic current is composed by four terms. The fourth one, i_p describes the sodium-potassium pump current. Therefore, the membrane current is given by: 2.14

$$i_m = c_m \frac{dV_m}{dt} + (i_{Na} + i_k + i_p + i_l) \quad (2.14)$$

and the individual ionic currents are expressed by the equations: 2.15 to 2.18 [1]

$$i_{Na} = \bar{P}_{Na} h m^2 \frac{EF^2}{RT} \frac{[Na]_o - [Na]_i e^{EF/RT}}{1 - e^{EF/RT}} \quad (2.15)$$

$$i_k = \bar{P}_k n^2 \frac{EF^2}{RT} \frac{[k]_o - [k]_i e^{EF/RT}}{1 - e^{EF/RT}} \quad (2.16)$$

$$i_p = \bar{P}_p p^2 \frac{EF^2}{RT} \frac{[Na]_o - [Na]_i e^{EF/RT}}{1 - e^{EF/RT}} \quad (2.17)$$

$$i_l = g_l (V_m - V_l) \quad (2.18)$$

Where

$$E = V_m + V_r \quad (2.19)$$

V_r is the resting potential.

The activation and deactivation variables m , n , h and p are governed by first-order differential equations 3.15 to 3.18:

$$\frac{dm}{dt} = \alpha_m(1 - m) - \beta_m m \quad (2.20)$$

$$\frac{dh}{dt} = \alpha_h(1 - h) - \beta_h h \quad (2.21)$$

$$\frac{dn}{dt} = \alpha_n(1 - n) - \beta_n n \quad (2.22)$$

$$\frac{dp}{dt} = \alpha_p(1 - p) - \beta_p p \quad (2.23)$$

Where α_i represent the i -th channel rate for switching from a closed to an open state while β_i that for switching from an open to a closed state. The α and β terms depend only on the transmembrane potential and are expressed by the equations 2.24 to 2.31 [1]:

$$\alpha_m = 0.36(V_m - 22) \left[1 - \exp\left(\frac{22 - V_m}{3}\right) \right]^{-1} \quad (2.24)$$

$$\beta_m = 0.4(13 - V_m) \left[1 - \exp\left(\frac{V_m - 13}{20}\right) \right]^{-1} \quad (2.25)$$

$$\alpha_h = 0.1(-10 - V_m) \left[1 - \exp\left(\frac{V_m + 10}{6}\right) \right]^{-1} \quad (2.26)$$

$$\beta_h = 4.5 \left[1 + \exp\left(\frac{45 - V_m}{10}\right) \right]^{-1} \quad (2.27)$$

<i>Constant</i>	<i>Value</i>	<i>Description</i>
\overline{P}_{Na}	$8 * 10^{-3} cm/s$	<i>Sodium permeability constant</i>
\overline{P}_k	$1.2 * 10^{-3} cm/s$	<i>Potassium permeability constant</i>
\overline{P}_p	$0.54 * 10^{-3} cm/s$	<i>Nonspecific permeability constant</i>
g_l	$30.3 mS/cm^2$	<i>Leakage conductance</i>
V_l	$0.026 mV$	<i>Leakage equilibrium potential</i>
$[Na]_o$	$114.5 mM$	<i>External sodium concentration</i>
$[Na]_i$	$13.7 mM$	<i>Internal sodium concentration</i>
$[K]_o$	$2.5 mM$	<i>External potassium concentration</i>
$[K]_i$	$12 mM$	<i>Internal potassium concentration</i>
F	$96.514 C/gmol$	<i>Faraday constant</i>
R	$8.3144 J/Kmol$	<i>Gas constant</i>
T	$295.18 K$	<i>Absolute temperature</i>
V_r	$-70 mV$	<i>Resting potential</i>
c_m	$2 \mu F/cm^2$	<i>Membrane capacitance per unit area</i>

Table 2.2: Constants for FH equations

$$\alpha_n = 0.02(V_m - 35) \left[1 - \exp \left(\frac{35 - V_m}{10} \right) \right]^{-1} \quad (2.28)$$

$$\beta_n = 0.05(10 - V_m) \left[1 - \exp \left(\frac{V_m - 10}{10} \right) \right]^{-1} \quad (2.29)$$

$$\alpha_p = 0.006(V_m - 40) \left[1 - \exp \left(\frac{40 - V_m}{10} \right) \right]^{-1} \quad (2.30)$$

$$\beta_p = 0.09(-25 - V_m) \left[1 - \exp \left(\frac{V_m + 25}{20} \right) \right]^{-1} \quad (2.31)$$

Specific constants for the FH equations are given in table 2.2

2.4 Action potential

After seeing the characteristics of the cell membrane of excitable cells, especially the functioning of the ion channels, let's see how these interact with each other. The ion channels interact through their common transmembrane potential and capacitance. A remarkable result is that such electrically active tissue, by means of a regenerative process, can generate a transient pulse of electrical changes, an action potential, across the cell membrane. The phenomenon of the action potential consists in a rapid depolarization of the membrane, i.e. an increase in the transmembrane potential, followed by a slower recovery of the resting condition. When an action potential occurs in a specific area of the membrane, the effect of depolarization is also felt in the adjacent areas and this causes other action potentials to arise which are then transmitted along the entire membrane.

When a stimulus of any kind occurs there is a change in the membrane potential, if this variation exceeds a threshold the sodium channels are activated and this causes a flow of sodium ions towards the inside of the cell. The flow of positive charges causes a rapid depolarization and the membrane potential increases rapidly until it reaches values of about $30 - 40\text{mV}$ this phase is called Depolarisation.

At 30 mV potassium channels begin to open and sodium channel gates close, in this phase, called Repolarization, there is a flow of potassium ions towards the outside of the cell which tries to bring the potential back to rest conditions. The potassium channels, however, are slow to close, consequently, the membrane potential continues to drop until it exceeds the initial value of -70 mV (Rest conditions) causing an undershoot. In the final phase it is the task of the sodium potassium pumps to bring the cell back to rest conditions, this phase is known as recovery period.

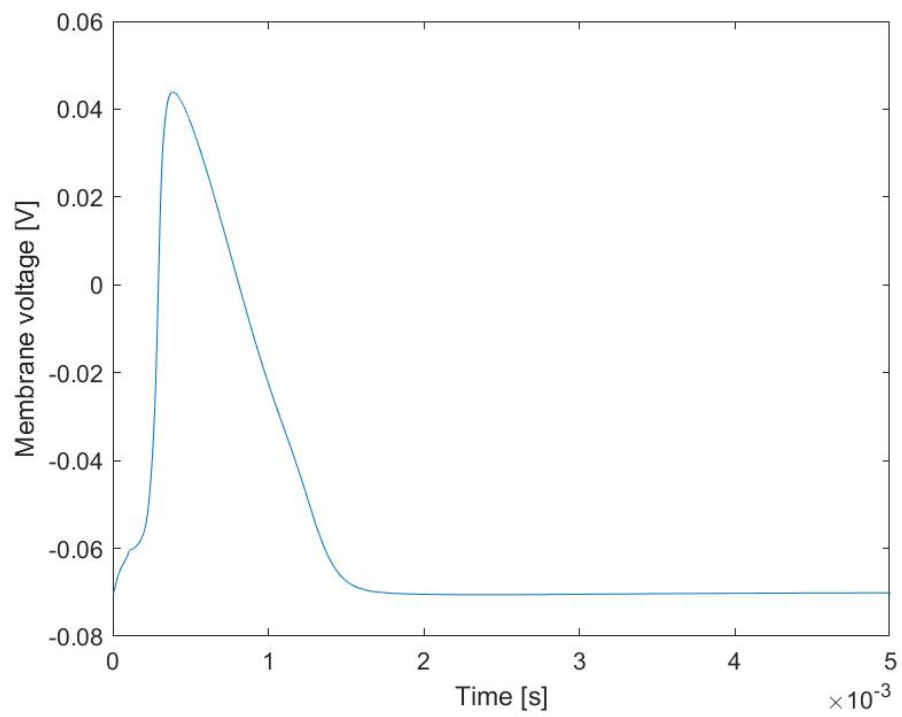


Figure 2.5: Action potential

Chapter 3

Impulse Propagation

In the previous chapters we discussed how an Action Potential is generated, we gave a mathematical representation of the excitable cells summaries in F-H equations. now we need to introduce a mathematical model to explain the impulse propagation from one node to an other.

To describe this phenomena we will refer to the Reilly's neuro-electric model "used" in [3] we replicated exactly his experiment and used his results to have a comparison. After that we will introduce our model that is an extension of the Reilly's one with the modification to include F-H non linear conductances on each node, we considered all nodes as non linear.

3.1 Mathematical model

In the current paragraph a generic mathematical representation is given. We can approximate a myelinated nerve with an electrical circuit as the shown in figure 3.1.

This representation is valid under some assumptions [3] and [2]; an infinitely long fiber is considered with Ranvier nodes that are regularly spaced, the external medium is uniform and isotropic, the internodal distance is proportional to the fiber diameter (D). Both axon diameter (d) and internodal gap (l) are proportional

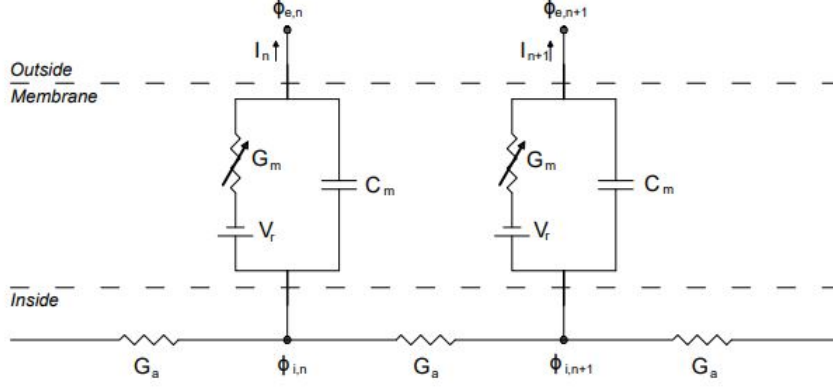


Figure 3.1: Circuit Model

to the fiber diameter. The myelin sheath is considered as a perfect insulator. The circuit parameters can be calculated as the following: The internodal conductance is given by:

$$G_a = \frac{\pi d^2}{4\rho_i L} \quad (3.1)$$

The membrane impedance is composed by the capacitor C_m in parallel to the conductance G_m that are given by:

$$C_m = c_m \pi dl \quad (3.2)$$

and

$$G_m = g_m \pi dl \quad (3.3)$$

Applying the KCL to a generic node k we get that the current at the node is equal to the sum of the incoming axial current, capacitive current and ionic current. in mathematical terms we can write:

$$C_m \frac{dV_k}{dt} + G_m V_k = G_a (\phi_{i,k-1} - 2\phi_{i,k} + \phi_{i,k+1}) \quad (3.4)$$

Where V_k is given by $\phi_e - \phi_i - V_r$, the first two terms are the external and internal potential respectively, with reference to a point within the external medium and far from the fiber. V_r is the rest potential. We suppose that the external potential is due only to the stimulus current and it is not influenced by the presence of the fiber.

Rearranging the equation we get the following [5]:

$$\frac{d\mathbf{V}_k}{dt} = \frac{1}{C_m} [\mathbf{G}_a (\mathbf{V}_{k-1} - 2\mathbf{V}_k + \mathbf{V}_{k+1} + \phi_{e,k-1} - 2\phi_{e,k} + \phi_{e,k+1}) - \mathbf{G}_m \mathbf{V}_k] \quad (3.5)$$

where: $(k = -n, \dots - 2, -1, 0, 1, 2, \dots, n)$.

3.5 is a set of first order differential equation that describe well myelinated fibers, initial conditions are considered to be $V_k(0) = 0$ thanks to the membrane capacitance that shunts the nodes.

The ionic term $I_{m,k} = G_m V_k$ is the responsible of the non linearity, as we saw in the previous paragraph $G_m = f(t, V_k)$, it depends on stimulus level. For sub-threshold stimuli G_m is considered constant and depending only on fiber diameter, in this case we have a linear set of differential equations. Generally speaking, I_n can be defined as:

$$\mathbf{I}_{m,k} = \begin{cases} G_m V_k \\ \pi dl(i_{Na} + i_k + i_p + i_l) \end{cases} \quad (3.6)$$

Using matrix notation the equation becomes:

$$[C_m] \frac{d}{dt} \{V\} = -[G_a](\{V\} + \{\phi_e\}) - [G_m]\{V\} \quad (3.7)$$

with: $[C_m]$ is the diagonal capacitance matrix

$$[C_m] = \begin{bmatrix} C_m^{11} & \cdot & 0 & 0 \\ \cdot & C_m^{ii} & \cdot & 0 \\ 0 & \cdot & \cdot & \cdot \\ 0 & 0 & \cdot & C_m^{nn} \end{bmatrix} \quad (3.8)$$

$[G_a]$ the internodale conductance matrix is given by the transpose of $[A]$ times $[G_a]$ times $[A]$. with $[A]$ edge-to-node incidence matrix.

$$[G_a] = [A]^T \begin{bmatrix} G_a^{11} & \cdot & 0 & 0 \\ \cdot & G_a^{ii} & \cdot & 0 \\ 0 & \cdot & \cdot & \cdot \\ 0 & 0 & \cdot & G_a^{nn} \end{bmatrix} [A] \quad (3.9)$$

$$[A] = \begin{bmatrix} -1 & 1 & \cdot & \cdot \\ \cdot & -1 & 1 & \cdot \\ \cdot & \cdot & -1 & 1 \\ \cdot & \cdot & \cdot & -1 \end{bmatrix} \quad (3.10)$$

$[G_m]$ in case of sub-threshold stimuli is a diagonal matrix.

$$[G_m] = \begin{bmatrix} G_m^{11} & \cdot & 0 & 0 \\ \cdot & G_m^{ii} & \cdot & 0 \\ 0 & \cdot & \cdot & \cdot \\ 0 & 0 & \cdot & G_m^{nn} \end{bmatrix} \quad (3.11)$$

Matrix notation is useful for the implementation of a Matlab code necessary to solving the problem numerically.

3.2 External Voltage Source ϕ_e

Both Reilly and McNeal represented the nerve fiber, for their experiments, as shown in figure 3.2. They considered a $20 \mu\text{m}$ -diameter fiber indefinitely long, having an internodal distance about 2mm . They used for the external stimulus a spherical electrode positioned above a Ranvier node¹ and placed at one internodal distance (20mm) from the fiber.

¹The electrode is positioned above the central Ranvier node, considering a symmetrical problem

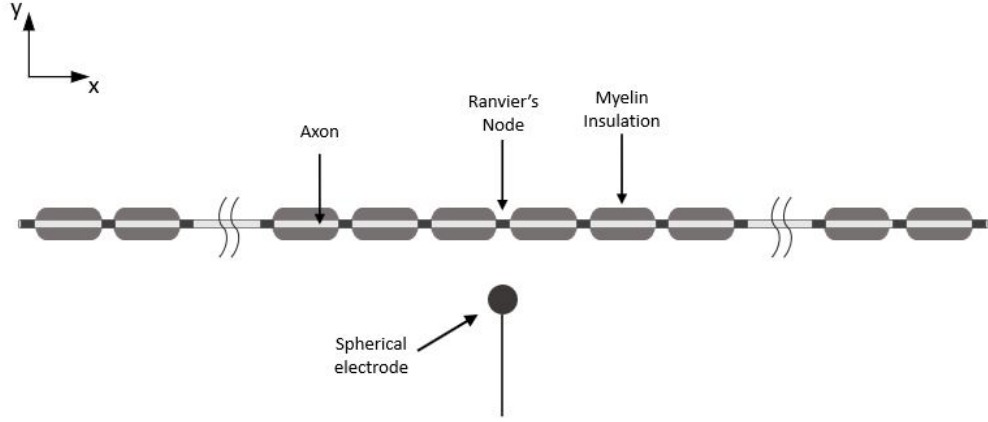


Figure 3.2: Nerve Model

The spatial distribution of the voltage along the axon, in the external medium, is a consequence of the stimulating current. It was assumed that the current propagates evenly from the electrode, in accordance with the hypothesis mentioned above, the potential at a distance r is given simply by equation 3.12.

$$\phi_e(t, r) = \frac{\rho_e I_x}{4\pi r} \quad (3.12)$$

Where ρ_e is the resistivity of the external medium and I_x is the stimulation current.

In this chapter we analyzed the model response to a rectangular stimulating pulse 3.13. A $100 \mu s$ pulse duration was considered with three different magnitudes; threshold stimuli I_t , sub-threshold stimuli $0.8I_t$ and supra-threshold stimuli $1.2I_t$ [3].

$$\mathbf{I}_x(\mathbf{t}) = \begin{cases} I_t; & 0 \leq t \leq 100\mu s \\ 0; & 100\mu s < t \end{cases} \quad (3.13)$$

3.3 Spatially Extended Nonlinear Node

Spatially Extended Nonlinear Node (SENN) model is the one used by Reilly [3] in his studies, this model is basically the Mc-

Neal's one [5] with the difference that Reilly considered as non-linear nodes, in addition to the stimulus node the one near the electrode, also an x number of adjacent nodes [3], consequently it was necessary to use Frankenhaeuser and Huxley conductances model at each non linear node.

the number of non-linear nodes to be used was limited by the computational power available in those years.

3.3.1 SENN Implementation

To replicate the Reilly's work a 21-node axon model was considered and implemented on Matlab using the same parameters shown in table 2.2 [3] [5], other geometric and electrical parameters are listed in the following table 3.1:

<i>Fiber diameter</i>	D	20 μm
<i>Axon diameter</i>	d	0.7 * D μm
<i>Internodal length</i>	L	100 * D μm
<i>Nodal gap width</i>	l	2.5 μm
<i>Axoplasm resistivity</i>	ρ_i	110 $\Omega.cm$
<i>External medium resistivity</i>	ρ_e	300 $\Omega.cm$
<i>Membrane conductance per unit area</i>	g_m	30.4 mS/cm^2
<i>Membrane capacitance per unit area</i>	c_m	2.5 $\mu F/cm^2$

Table 3.1: Input Parameters

The set of differential equations that was implemented for the non-linear nodes is the following 3.14:

$$\frac{dV_k}{dt} = \frac{1}{C_m} [G_a (V_{k-1} - 2V_k + V_{k+1} + \phi_{e,k-1} - 2\phi_{e,k} + \phi_{e,k+1}) - \pi dl(i_{Na}(h, m, V) + i_k(n, V) + i_p(p, V) + i_l(V))] \quad (3.14)$$

In addition there are 4 equations for each nonlinear node:

$$\frac{dm}{dt} = \alpha_m(1 - m) - \beta_m m \quad (3.15)$$

$$\frac{dh}{dt} = \alpha_h(1 - h) - \beta_h h \quad (3.16)$$

$$\frac{dn}{dt} = \alpha_n(1 - n) - \beta_n n \quad (3.17)$$

$$\frac{dp}{dt} = \alpha_p(1 - p) - \beta_p p \quad (3.18)$$

Regarding the initial conditions, the following values were used [5]:

$$V_k(0) = 0; \quad \forall k$$

$$h(0) = 0.8249;$$

$$m(0) = 0.0005;$$

$$n(0) = 0.0268;$$

$$p(0) = 0.0049;$$

The threshold current needed for the stimulus was calculated using bisection method: the set of differential equations mentioned above was solved iterating different stimulus current values until the membrane voltage of at least three nodes exceeds $80mV$. The threshold stimulus pulse I_t calculated, corresponds to the same one used by Reilly [3] and it is negative $0.68mA$.

3.3.2 SENN Model Results

As mentioned before, three different kind of stimuli were analyzed: a sub-threshold stimulus with a current value about 80% of the threshold and a supra-threshold stimulus with a current value that corresponds to 120%.

Referring to the figure 3.2, the nearest node to the electrode is the eleventh one, it is the one with maximum excitation. In figure 3.3 we can observe the node response to a sub-threshold stimulus. As we note, it is simply a passive RC circuit response.

The stimulus value is not sufficient to generate an action potential, consequently, the effect on the adjacent nodes is negligible as we can see in figure 3.4.

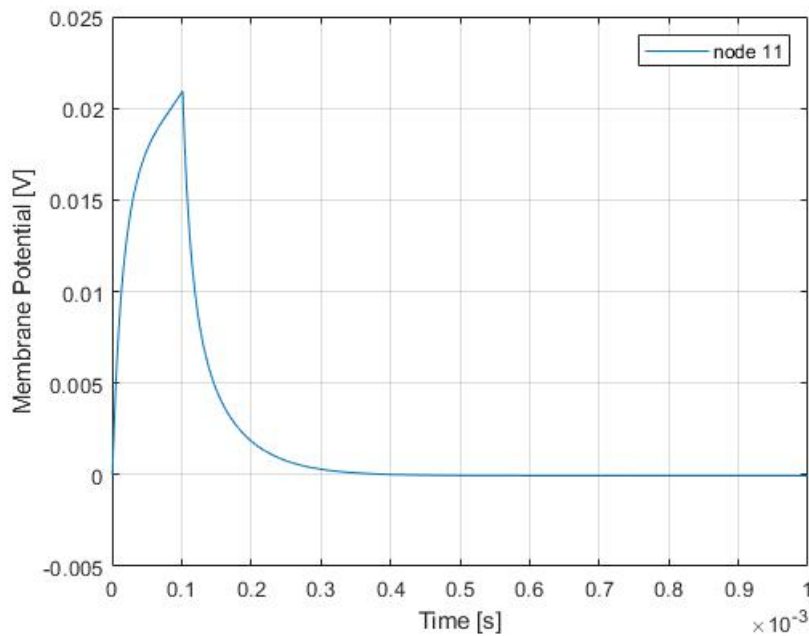


Figure 3.3: Sub-threshold response

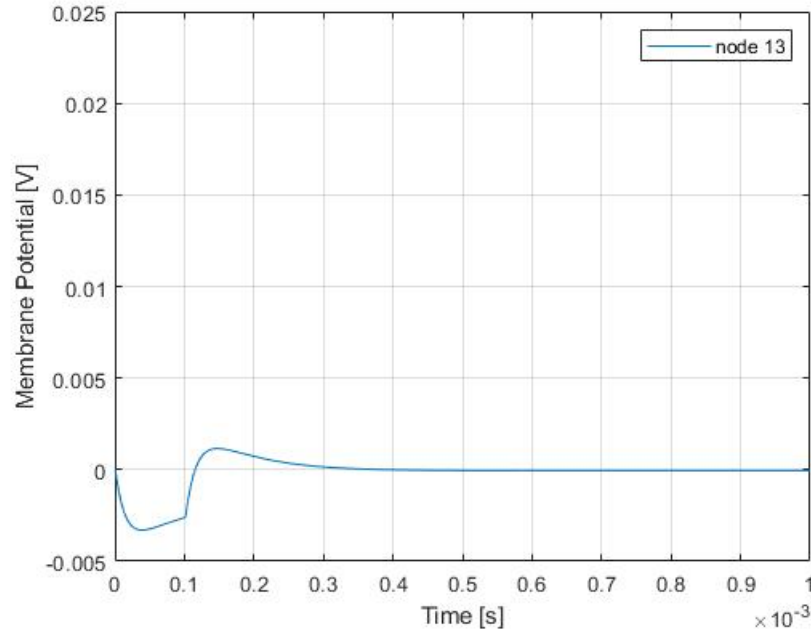


Figure 3.4: Node-13 Sub-threshold response

In the following figures we can see the response to the threshold current. The eleventh node, as we said, is the nearest to the electrode, consequently, is where the action potential is generated. As described in the previous chapter, when the membrane potential reaches $30mV$ the sodium channels are activated causing an ions flow towards the inside of the cell, this flow causes a rapid depolarisation as shown in figure: 3.5. The membrane voltage increases until exceeding $100mV$, after that potassium channels open bringing back the potential to the initial value.

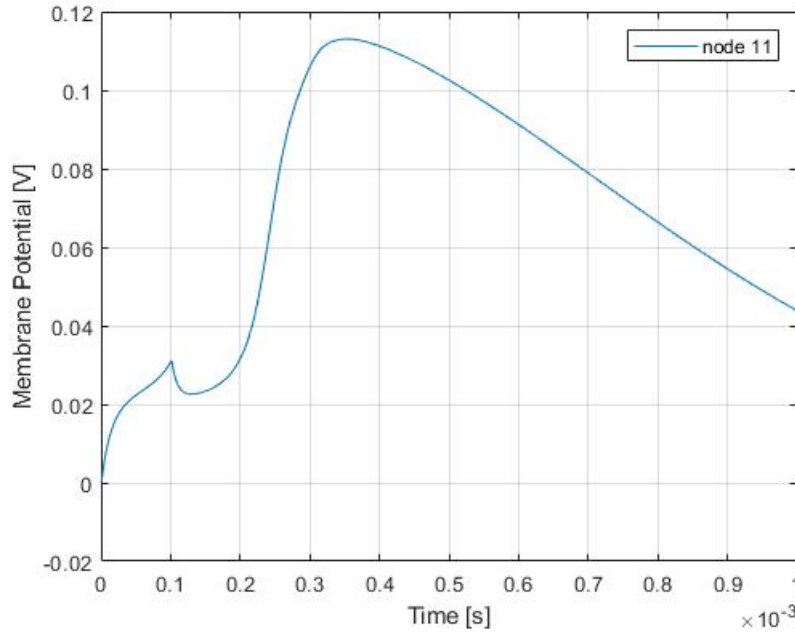


Figure 3.5: Node-11 threshold response

The figure 3.6 shows the response of the three adjacent nodes: twelfth, thirteenth and fourteenth. The same result was obtained by Reilly [3].

We can notice a little time delay between the three curves due to the finite propagation velocity, that it's supposed to be about $60m/s$ [3] for mammalian fibers. In this work the propagation velocity is about $40m/s$, this difference is a consequence of the low temperature considered in the Frankenhaeuser and Huxley equations.

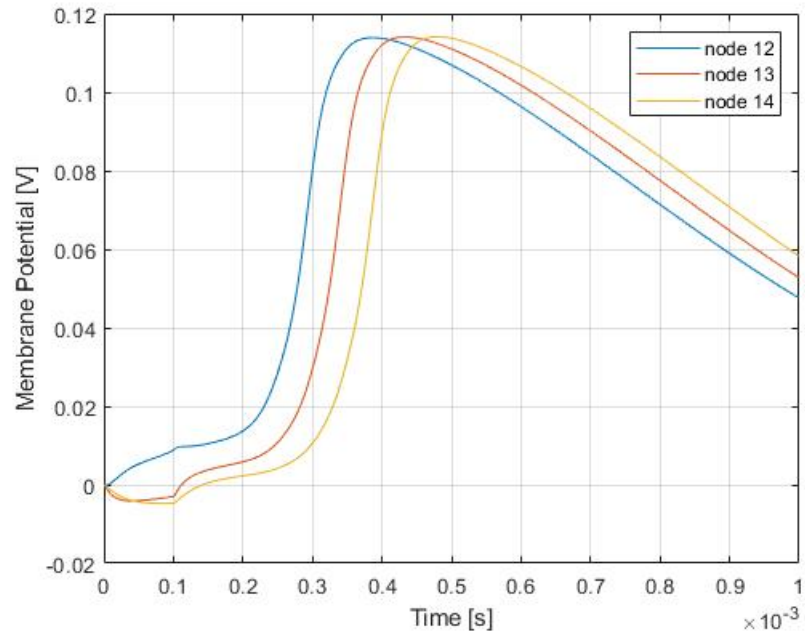


Figure 3.6: adjacent nodes threshold response

Finely, in figure 3.7 we have the response of the eleventh node to a supra-threshold stimulus. We notice that the depolarisation is much rapid compared to the previous case,

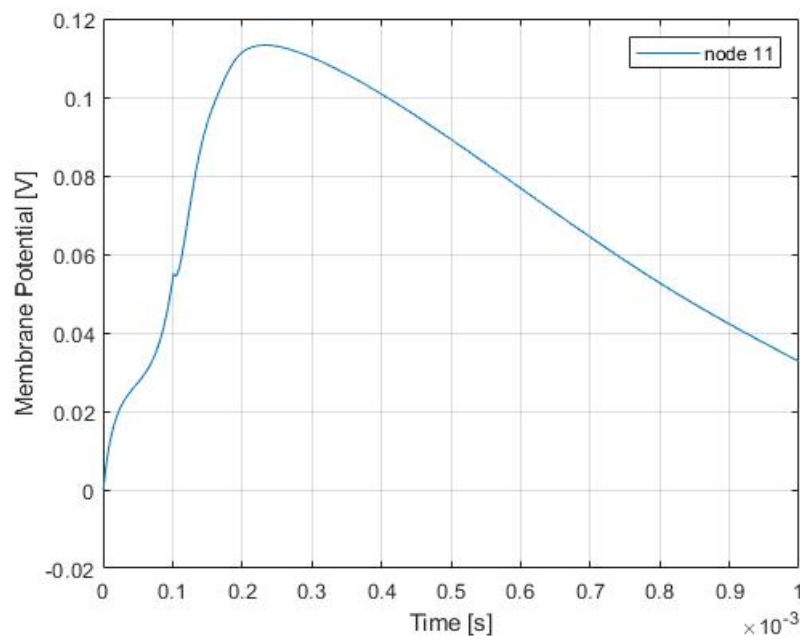


Figure 3.7: Node-11 Supra-threshold response

Chapter 4

Model Simulation

In the current chapter we modified the SENN model introducing non-linear Frankenhaeuser and Huxley conductances at each node of our nerve model, we implemented a compact Matlab code that solves many classes of nerve structures with different stimulus sources. We solved the same 1D-nerve model as Reilly to compare the results obtained.

After that we defined a 3D-cylinder model to simulate human body parts, we focused only on the geometric features considering uniform electrical proprieties of each tissue. We applied our neuroelectric model to a single branched nerve structure contained within the cylinder.

We studied the case of a discrete voltage distribution given by two different sources. In one case we considered a voltage distribution generated by two electrodes, the other case regards a distribution of electrical field generated by a source external to the body.

4.1 modified SENN

In the previous chapter we defined a mathematical model in matrix notation 3.7 for the linear case, we can use the same formalism for a most general form that works for both linear and non linear nodes 4.1.

$$\begin{aligned} \begin{bmatrix} [C_m] & 0 \\ 0 & [I_d] \end{bmatrix} \frac{d}{dt} \begin{Bmatrix} \bar{V} \\ \tilde{a} \end{Bmatrix} = - \begin{bmatrix} [G_a] & 0 \\ 0 & (\bar{\alpha}^T + \bar{\beta}^T)[I_d] \end{bmatrix} \begin{Bmatrix} \bar{V} \\ \tilde{a} \end{Bmatrix} + \\ + \begin{bmatrix} [G_a] & 0 \\ 0 & [I_d] \end{bmatrix} \begin{Bmatrix} \bar{\phi}_e \\ \bar{\alpha} \end{Bmatrix} + S \begin{Bmatrix} \bar{I}_m \\ 0 \end{Bmatrix} \quad (4.1) \end{aligned}$$

Where: $[G_a]$, $[C_m]$ are the $N \times N$ matrixes defined in Chapter 3 and $[I_d]$ is the $4N \times 4N$ identity matrix, with N the total node number.

$\bar{\alpha}_k = [\alpha_m \ \alpha_h \ \alpha_n \ \alpha_p]^T$ and $\bar{\beta}_k = [\beta_m \ \beta_h \ \beta_n \ \beta_p]^T$ are the arrays containing the switching rates as mentioned previously 2.24 to 2.31.

\bar{I}_m is the membrane current density array and $S = \pi dl$.

$\tilde{a} = [m_1 \ h_1 \ n_1 \ p_1 \ \cdots \ m_k \ h_k \ n_k \ p_k \ \cdots \ m_n \ h_n \ n_n \ p_n]^T$ is the array containing the activation variables defined in Chapter 2.

\bar{V} and $\bar{\phi}_e$ are the membrane voltage and the external potential respectively.

The set of non linear differential equations 4.1 has the classic form: $M\dot{y} = f(t, y)$, it was implemented on Matlab and solved using the "ode23t" algorithm. The choice of the algorithm is based on the fact that the mass matrix " M ", in some cases, can be singular and in these cases the problem becomes "DAE" Differential-Algebraic Equation instead of Ordinary Differential Equation. The "ode23t" solves moderately stiff ODEs and DAEs using a trapezoidal rule. In the next paragraph a brief description of the code is given.

4.1.1 Code Implementation

The ode23t solver needs as inputs a function handle defined as $\dot{y} = f(t, y)$, the time interval of integration $[T_0 \ T_{final}]$, the position and number of Ranvier's nodes in addition to the internodale

conductance matrix. The ode function returns a colon vector that corresponds to $f(t, y)$.

```
function dy=Ffun(t,y,Ga,P,Q,nNod)

%
% OUTPUT
%   system of differential equations y' = f(t,y)
% -----
% INPUTS
%       Ga : Internodale conductance matrix
%       P   : Node coordinates
%       Q   : Electrodes position
%       nNod: Number of nodes
% -----
%
% ----- Version 1.0 -----
%       Created: 2021-04-11
% -----

d = evalin('base', 'd');      % d = 0.7*D;
l = evalin('base', 'l');      % l = 2.5e-6;

v=y(1:nNod);
m=y(nNod+1:4:5*nNod-3);
h=y(nNod+2:4:5*nNod-2);
n=y(nNod+3:4:5*nNod-1);
p=y(nNod+4:4:5*nNod);

dy(1:nNod,1)=-Ga*v-Ga*sourcePotential(t,Q,P)-pi*d*l*(iNa(h,m,v)+iK(n,v)+iP(p,v)+iL(v));
dy(nNod+1:4:5*nNod-3)=alpham(v).*(1-m)-betam(v).*m;
dy(nNod+2:4:5*nNod-2)=alphah(v).*(1-h)-betah(v).*h;
dy(nNod+3:4:5*nNod-1)=alphan(v).*(1-n)-betan(v).*n;
dy(nNod+4:4:5*nNod)=alphap(v).*(1-p)-betap(v).*p;

end
```

The following code is the main one where the "ode" solver is called. It was decided to structure the code by dividing it into many functions¹ that can be independently modified according to needs.

```
clear variables, close all
%%
% initialize variables
Init_var;

% nerve description
load nerve_structure

nNod = size(Pn,1);          %nNod: number of Ranvier nodes, Pn: nodes coordinates
nEdg = size(En,1);          %nEdg: edges number
jcol = abs(En,');           %
irow = repmat(jcol(1,:),2,1); %
```

¹only two examples have been reported so as not to burden the discussion too much

```

s = sign(En. ');

% electrode position (Excitation Model)
Define_electrode_pos;

%Matrixes construction
A = sparse(double(irow(1:end-1)),double(jcol(1:end-1)),double(s(1:end-1))); %edge-to-node
    incidence matrix
Ga = pi * d ^ 2 ./ (4 * rhoi * Inter_d); %internodale conductance
Ga = A.'*spdiags(Ga,0,nEdg)*A; %internodale conductance matrix
Cm = sparse(1:nNod,1:nNod,Cm_p*ones(1,nNod),nNod,nNod); %Membrane capacitance matrix
Cm_NL = sparse(blkdiag(Cm,eye(4*nNod))); %Mass Matrix

%Initial conditions
x0 = [zeros(1,nNod) repmat([5e-4, 0.8249, 0.0268, 0.0049],1,nNod)]; %Inizial conditions

% ode solution
options = odeset('Mass',Cm_NL,'MassSingular','yes','MStateDependence','none',...
'RelTol',1e-6,'AbsTol',1e-6);
[t,y] = ode23t(@(t,y)Ffun(t,y,Ga,Pn,Q,nNod),tSpan,x0,options);

```

4.2 Modified SENN application

4.2.1 21-node axon model response

At first, the modified SENN was tested on the same 21-node axon model as the one used by Reilly to make a comparison. The same experiments were replicated using exactly the same data.

Three stimulus cases were analyzed: sub-threshold stimulus, threshold stimulus and a sopra-threshold stimulus, with 80%, 100% and 120% respectively of the stimulus current I_t . Regarding the first two cases, in correspondence with the non-linear nodes, i.e. the stimulus one plus the adjacent nodes, the response are exactly equals since the same equations were used. On the other hand, the difference can be observed in the case of the sub-threshold response, as shown in figure 4.1, a consequence of the fact that in one model a simple RC circuit is used, while in the other the non-linear F-H equations are used.

It can be noted that the response of the linear model is slightly underestimated, it has a maximum deviation of approximately 5% at node 11, the one with the highest stimulus value due to

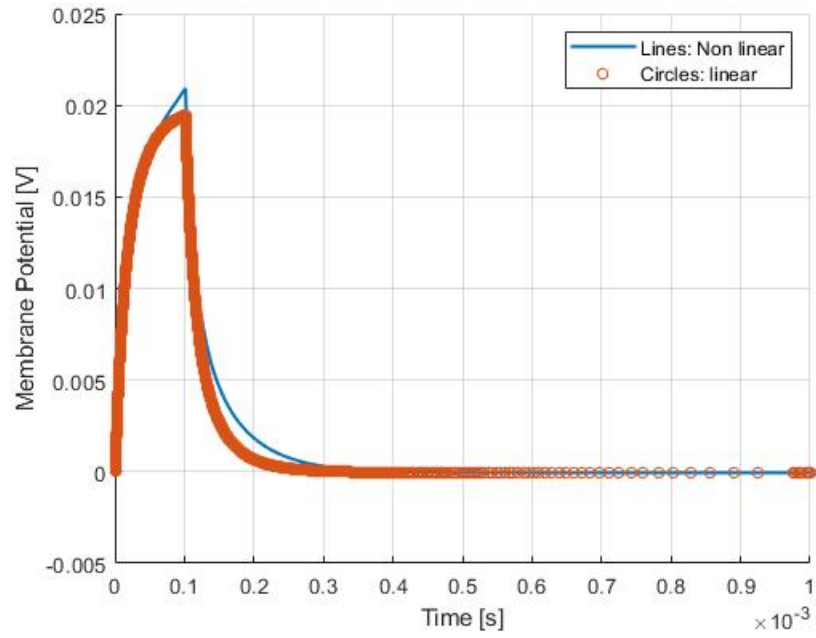


Figure 4.1: Node-11 linear vs nonlinear comparison

its proximity to the electrode. The following figure 4.2 shows the trend of the membrane voltage of the next 4 adjacent nodes.

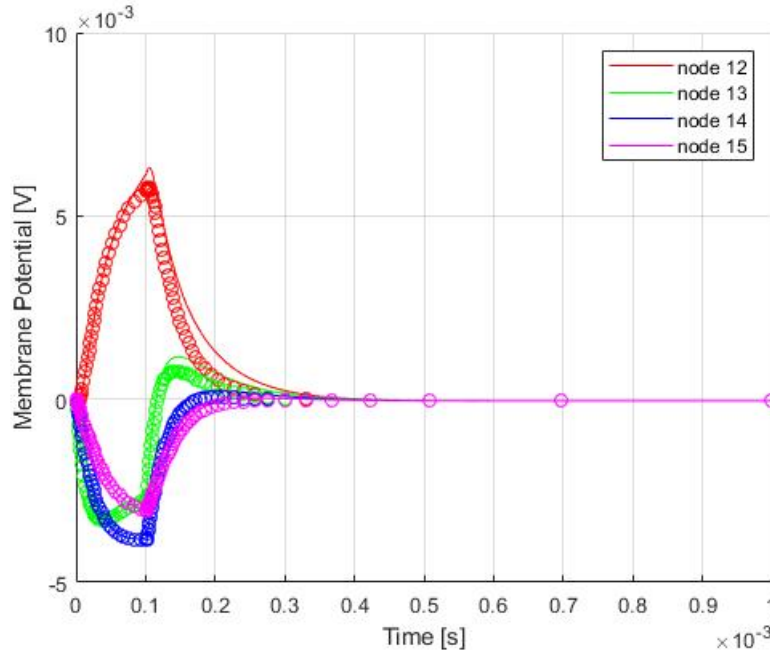


Figure 4.2: Nodes 12 to 15 comparison, lines: nonlinear; circles: linear

4.2.2 3D-body model

In order to model the nerve stimulation in the body induced by an external magnetic field, it is necessary to have a 3D representation of the body in addition to the spatial distribution of the magnetic field. The approach used in this thesis work is that to represent a part of the body, which can be an arm or a leg, using simple geometries, in particular concentric homogeneous cylinders each of which represents a biological tissue (bones, muscles, fat and skin) as shown in figure 4.3. The nerves have been schematized with a structure having a main nerve that branches in two others obtaining an inverted Y shape as shown in the figure 4.4. The electrical proprieties of the tissues were considered constant.

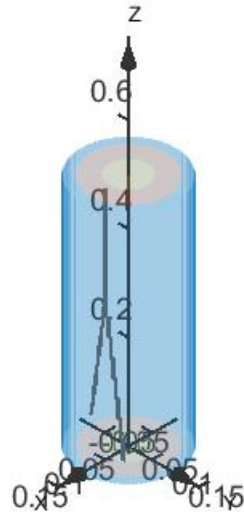


Figure 4.3: 3D-Cylinder Model

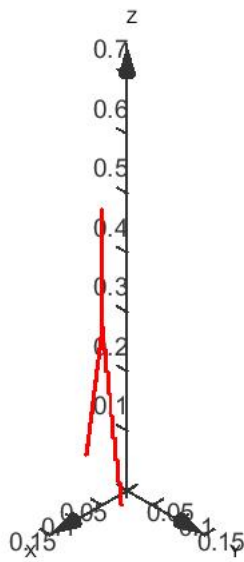


Figure 4.4: 3D-Cylinder Model

4.2.3 Y-model response

From the 3D voxel model the structure of the nerve was extracted, after which its center-line, figure 4.5, was identified using a skeletonization algorithm. The purpose of using the skeleton is to maintain the topological properties of the structure.

Figure² 4.5 shows, in addition to the exact position of the nerves, also the position of the spherical electrode needed to inject the stimulus current.

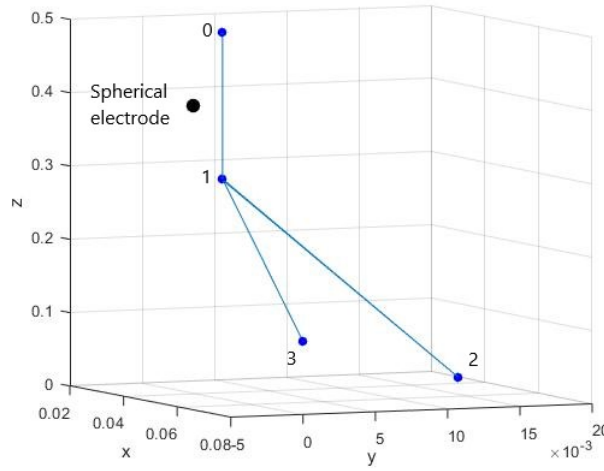


Figure 4.5: Y Model skeleton

The structure can be treated as a graph having 4 nodes, numbered from 0 to 4 and connected to each other by three branches: (0-1), (1-2) and (1-3). In each branch the Ranvier nodes present were calculated with the constraint of having an internodal distance equal to 20 mm, with this condition we get 100 nodes for the first branch (0-1), 150 and 101 for second (1-2) and third (1-3) ones respectively, with a total of 351 Ranvier nodes. Two new matrixes were created: $[P_n]$ containing the position of each node and the connectivity matrix $[E_n]$ which defines the connections

²the nerve model is the same as shown in figure 4.4 but from a different view to highlight the position of the electrode

between Ranvier nodes.

The $[E_n]$ is a $N \times 2$ matrix with N the total node number, each row represents a branch, the first element of the row is starting node while the second is the arrival one. Thanks to $[E_n]$ it was possible to construct the edge-to-node incidence matrix $[A]$ defined in 3.10 and consequently also internodale conductance matrix $[G_a]$ as 3.9.

Regarding the external potential ϕ_e it was given by a spherical electrode, the same described in the previous chapter. The electrode was positioned, as shown in figure 4.5, at node 50 of the first branch. The distance between the electrode and the nerve is 20 mm, equal to the internodal distance.

After defining all the terms of the mathematical model 4.1 we solved the set of differential equations using the same Matlab ode solver the "ode23t", the same adopted for the solution of the 21-node axon model described previously. We analysed the three different cases of external stimulus: sub-threshold, threshold and sopra-threshold stimuli, using the same value of excitation current as in the cases analyzed above.

The results of the calculations are shown in the following figures:

The figure 4.6 shows the result of sub-threshold stimulus, as expected, the trend follows that of an RC circuit, the same result was obtained by Reilly as we shown in the previous chapter.

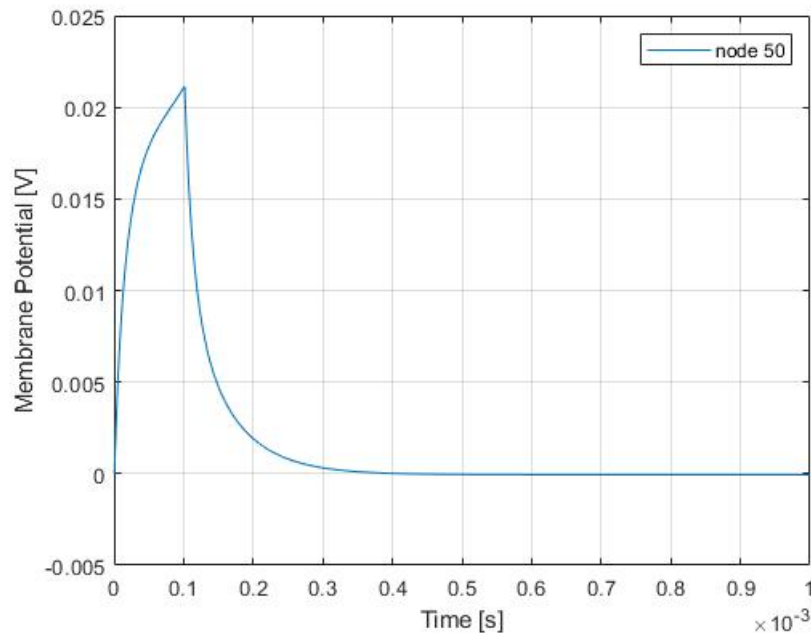


Figure 4.6: Sub-threshold stimulus result

The next figure: 4.7 shows the threshold stimulus, there is no change between this one and the result obtained by Reilly.

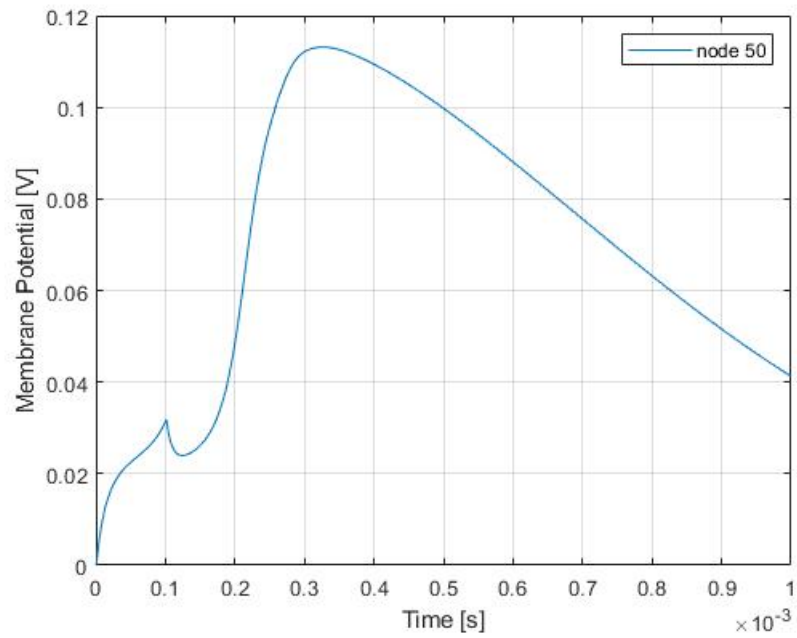


Figure 4.7: Threshold stimulus result

Also for the supra-threshold stimuli we can say the same thing, that because the only difference between two models is that in this case we have a large number of points.

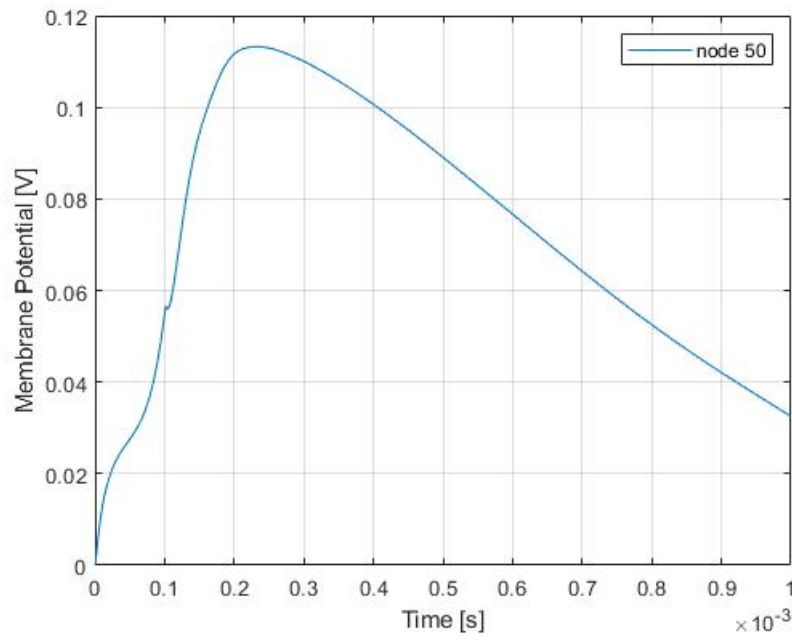


Figure 4.8: sopra-threshold stimulus result

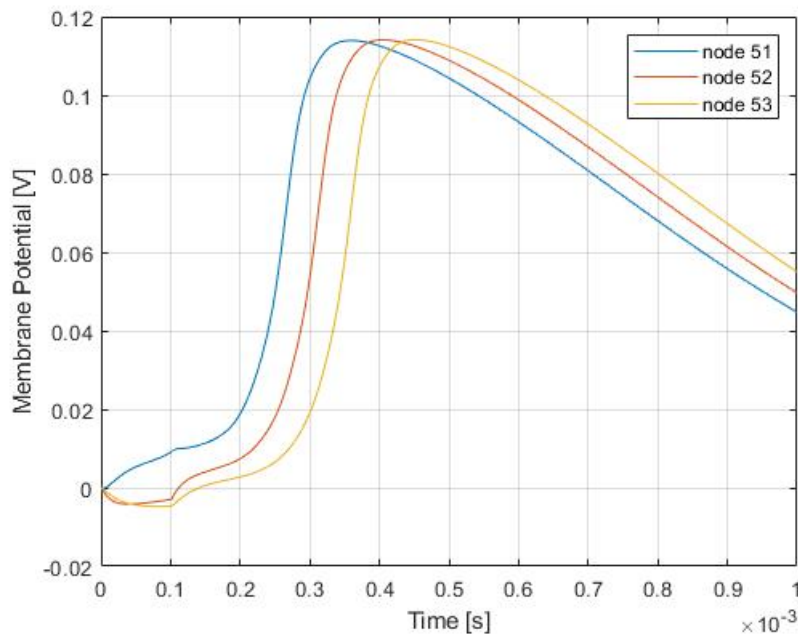


Figure 4.9: Adjacent nodes - sopra-threshold stimulus result

One thing we can notice is that the distant nodes of the electrode do not feel the effect of the generated action potential as we can notice in figure 4.10

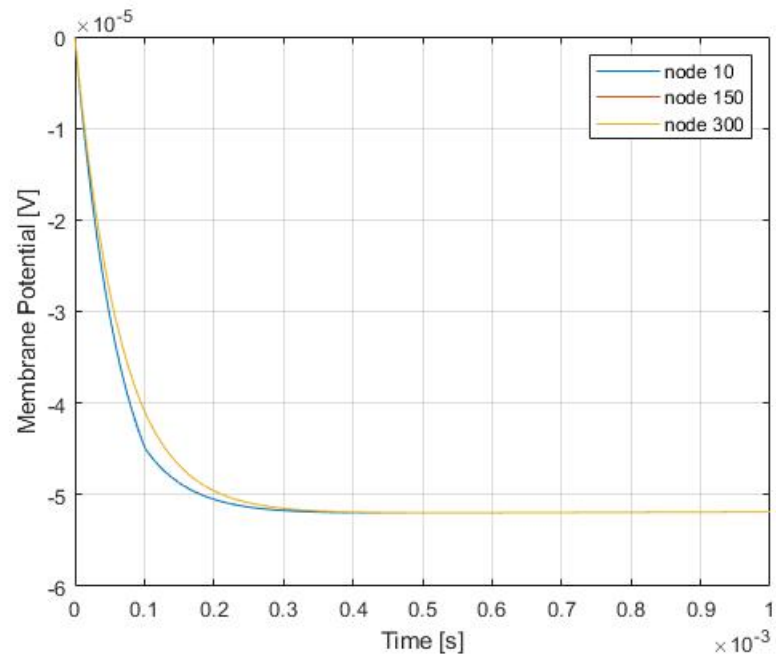


Figure 4.10: distant nodes

Chapter 5

3D Modeling

In order to simulate PNS (peripheral nerve stimulation) in a 3D object, that could be a complete real body model, or, in our case, a simplified representation of body part using simple geometries (like a cylindrical geometry), it is necessary to follow some steps. First of all we need to make a consideration: 3D models are usually found available in the form of a volumetric data-set containing the object properties with a voxel discretization¹. Each voxel, of finite size, contains the individual properties of the object residing in the unit of volume represented by that voxel.

As a first step, it is necessary to identify and extrapolate the voxels that represent the nervous system, or, as in our case, an equivalent nerve representation, from the entire 3D model. After that, using image processing algorithms, it is possible to calculate the center line that emphasizes the geometrical and topological properties of the nerves shape, to get a 1-D line representation of the 3-D object. As a last step, we evaluate the neurodynamic model described in the previous chapter to get the response of the nerve fiber to a predefined external electric potential.

¹[...] "Voxel is an image of a three-dimensional space region limited by given sizes, which has its own nodal point coordinates in an accepted coordinate system, its own form, its own state parameter that indicates its belonging to some modeled object, and has properties of modeled region." [8] (the voxel is the three-dimensional counterpart of the two-dimensional pixel)

5.1 Medial Axis

The medial axis (or skeleton) of an object is the locus of points with the property of being equidistant from its boundary. The skeleton conserves geometrical and topological properties of the object shape, such as topology, direction, length and connectivity. Skeleton, in addition to the distance of its points to the boundary, is used to represent object's shape.

A mathematical definition is given by Anil K.[4]:

" A disk (or ball) B is said to be maximal in a set A if:

- $B \subseteq A$, and
- If another disc D contains B , then $D \not\subseteq A$.

One way of defining the skeleton of a shape A is as the set of centers of all maximal disks in A ."

In literature there are many skeletonization algorithms that reduce a 3-D object to its skeleton without changing its topology. We can find three families of algorithm [9]: distance transform field-based methods, Voronoi diagram-based methods and thinning-based methods.

5.2 Skeletonization algorithm

For this thesis work we opt for a parallel thinning-based method that uses GPU processors for the center line extraction. The code take as input binary 3-D volume and creates a set of curvilinear segments that represent the skeleton of the 3-D shape. These algorithms are applied in various disciplines such as computer graphics, artificial intelligence, biology and medicine.

Thinning algorithm works basically by removing the external layer of the object until only one pixel thin center lines are remaining, preserving the topology of the object. A voxel " v " can be removed from the boundary of the 3-D binary image provided that it satisfies the following assumptions [9]:

- "v" has exactly one 26-connected object component in its 26-neighborhood,
- "v" one 6-connected background component, in its 18-neighborhood, which is 6-connected to p, and
- "v" has at least one 6-connected background neighbor.

A pair of voxel v_1 v_2 are called 6-connected if $d(v_1, v_2) = 1$, 18-connected if $d(v_1, v_2) = 2$ and 26-connected if $d(v_1, v_2) = 3$, where $d(.,.)$ indicates the Manhattan distance².

For more details on the 3-D thinning algorithms we refer the reader to [9].

²Manhattan distance between two points is the sum of the absolute differences of their Cartesian coordinates.

$$d(P, Q) = \sum_{n=1}^n |p_i - q_i|,$$

where P and Q are vectors

$P = (p_1, p_2, \dots, p_n)$ and $Q = (q_1, q_2, \dots, q_n)$

Chapter 6

Conclusion

In conclusion, the code obtained at the end is composed of many independent functions that call each other, the functions can be modified separately to allow you to analyze different types of stimulus and test the model on various 3-D geometries. The ease of implementation pays off in terms of computational cost, especially in the case of analysis of complex geometries with non-uniform induced electric field distributions, the calculation times increase greatly

To conclude, these models can be applied in various fields of research, it can be said that the work presented can be considered a starting point for developing more performing and efficient algorithms. It is quite easy to be able to test the model developed on a 3-D human body, the only criticality is the limited availability of detailed 3-D models. The next step is to test the model on a real case of exposure to electromagnetic fields using a real measurements.

Bibliography

- [1] A. F. HUXLEY B. FRANKENHAEUSER. “The action potential in the myelinated nerve fiber of *Xenopus Laevis* as computed on the basis of voltage clamp data”. In: *J. Physiol* 171 (1964), pp. 302–315.
- [2] RICHARD FITZHUGH. “Sensory Effects of Transient Electrical Stimulation - Evaluation with a Neuroelectric Model”. In: *Biophys.J.* 2.12 (1962), p. 11.
- [3] VANDA T. FREEMAN J. Patrick Reilly. “Sensory Effects of Transient Electrical Stimulation - Evaluation with a Neuroelectric Model”. In: *IEEE TRANSACTIONS ON BIOMEDICAL ENGINEERING* BME-32.12 (Dec. 1985).
- [4] Anil K. Jain. *Fundamentals of digital image processing*. Englewood Cliffs, NJ : Prentice Hall, 1989.
- [5] DONALD R. MCNEAL. “Analysis of a Model for Excitation of Myelinated Nerve”. In: *IEEE TRANSACTIONS ON BIOMEDICAL ENGINEERING* BME-23.4 (July 1976).
- [6] J. Patrick Reilly. *Applied Bioelectricity*. Vol. 1. 1998.
- [7] Roger C. Barr Robert Plonsey. *Bioelectricity A Quantitative Approach*. Vol. 3. 2007.
- [8] Catherine Igorevna Shchurova. “A methodology to design a 3D graphic editor for micro-modeling of fiber-reinforced composite parts”. In: *Advance in Engineering software* 90 (Dec. 2015), pp. 76–82.
- [9] Jin Xun and Jong-Weon Kim. “A 3D Skeletonization Algorithm for 3D Mesh Models Using a Partial Parallel 3D Thinning Algorithm and 3D Skeleton Correcting Algorithm”. In: *Applied Sciences* 7 (Feb. 2017), p. 139. DOI: 10.3390/app7020139.